



---

*Research article*

## **Fixed-time command filtered output feedback control for twin-roll inclined casting system with prescribed performance**

**Dongxiang Gao<sup>1</sup>, Yujun Zhang<sup>1,\*</sup>, Libing Wu<sup>2</sup> and Sihan Liu<sup>1</sup>**

<sup>1</sup> School of Computer and Software Engineering, University of Science and Technology Liaoning, Anshan, Liaoning, CO 114051, China

<sup>2</sup> School of Science, University of Science and Technology Liaoning, Anshan, Liaoning, CO 114051, China

\* **Correspondence:** Email: 865058381@qq.com; Tel: +86-138-8974-8068.

**Abstract:** The article investigates the issue of fixed-time control with adaptive output feedback for a twin-roll inclined casting system (TRICS) with disturbance. First, by using the mean value theorem, the nonaffine functions are decoupled to simplify the system. Second, radial basis function neural networks (RBFNNs) are introduced to approximate an unknown term, and a nonlinear neural state observer is created to handle the effects of unmeasured states. Then, the backstepping design framework is combined with prescribed performance and command filtering techniques to demonstrate that the scheme proposed in this article guarantees system performance within a fixed-time. The control design parameters determine the upper bound of settling time, regardless of the initial state of the system. Meanwhile, it ensures that all signals in the closed-loop system (CLS) remain bounded, and it can also maintain the tracking error within a predefined range within a fixed time. Finally, simulation results assert the effectiveness of the method.

**Keywords:** twin-roll inclined casting; fixed-time control; output feedback; prescribed performance; command filter

---

### **1. Introduction**

The twin-roll inclined casting and rolling process has widespread use in modern industrial production. Compared to traditional rolling processes, the elimination of initial rolling, heating, and other processes significantly shortens the production process, improves speed, reduces equipment investment, energy consumption, environmental pollution, and enhances the sheet's properties. Therefore, it is widely used in steel production with higher requirements for strength, toughness, and precision [1–4]. However, multiple coupled rolling parameters affect the rolling effect, making the precise control of

twin-roll inclined casting and rolling more challenging. In addition, controlling the stability time of the casting and rolling system and accelerating the convergence speed of errors are also key to optimizing system performance. To solve these problems, further research and improvement of this process are needed, and effective measures must be taken to ensure the controllability and stability of the rolling process.

In recent years, numerous scholars have proposed adaptive control schemes for practical engineering applications [5–8]. As shown in [5], Zhang et al. used the implicit function theorem and the mean value theorem to handle the nonaffine coupling term in the twin-roll inclined casting system (TRICS), which ensured that multi-input and multi-output (MIMO) nonaffine nonlinear systems could be converted into corresponding affine nonlinear systems. Furthermore, in order to avoid the impact of parameter uncertainty on the control effect for a type of nonlinear system for which it is difficult to measure its state, some neural networks (NNs) or fuzzy output feedback control strategies are proposed in [9–13]. These studies have propelled the development of adaptive control theory.

Although the aforementioned studies have significant implications, the control schemes designed were all discussed under infinite time intervals. However, in practical applications, the time required for the stability of the engineering system is an important consideration. As we have already known, Bhat and Bernstein proposed the finite-time control theory in [14], which brought the control of system stability within a finite time for the first time, and improved system robustness, convergence speed, and accuracy. Building on this pioneering work, numerous results have been developed using classical finite-time stability theory, which were later applied in a variety of control systems. For instance, adaptive finite-time control methods for uncertain nonlinear systems were investigated in [15–17]. A finite-time control scheme for stochastic nonlinear systems was proposed in [18]. The problem of adaptive and finite-time decentralized control for large-scale and nonlinear systems with input saturation and time-varying output constraints is addressed by [19].

Notably, finite-time control method's stabilization time is dependent on the initial state of the system under consideration, which is often challenging to acquire directly in various engineering systems. Consequently, designers face difficulties precisely predicting the time required for stabilization, limiting the application of finite-time control. To compensate for this shortcoming, Polyakov first proposed the fixed-time control theory in [20], whereby the stabilization time, solely based on the design parameters of the system, is independent of the system's initial state. Based on [20], research on fixed-time control has been continuously developed. Some such examples were discussed in [21, 22], which described research on the fixed-time tracking control issues in uncertain nonlinear systems. Additionally, [23] investigated the output feedback control design problem for nonlinear systems with full state constraints, based on a fixed-time state observer.

However, most of the above-mentioned studies focus only on the steady-state performance, which guarantees that the tracking error converges to a near-zero neighborhood, but transient performance has rarely been considered. Referring to the predetermined performance control scheme proposed in [24–26], it is known that the transient performance of the system is also extremely important in practical applications. Thus, optimizing the transient performance of the twin-roll inclined caster is critical for enhancing the overall performance of TRICS.

Based on the literature survey above, this paper proposes a fixed-time adaptive output feedback control strategy for TRICS with disturbance. The NNs state observer is designed to handle the influence of parameter uncertainties and unmeasurable states on stability. To solve the differential explosion and

singularity problem caused by the virtual control function in the backstepping design, a command filter is introduced. In addition, combined with the predetermined performance theory, it can simultaneously ensure the steady-state and transient performance of the system. The constructed fixed-time controller can guarantee that all signals in the CLS are bounded, and the tracking error of the output signal can converge to a predefined set within a fixed time.

The following are the primary contributions of this research:

1) In [5–7], the state variables regarding the control strategy of TRICS are assumed to be measurable. However, in reality, the rate of change of the TRICS molten pool level is often unmeasurable. Therefore, the control scheme proposed in [5–7] cannot be effectively implemented in practice. In this paper, we construct the NNs state observer to compensate for parameter uncertainty and the effect of unmeasured states on TRICS.

2) For the control results in [5–7], only the stability of TRICS under infinite time conditions is considered. However, in practice, setting a stable convergence time for the system is also crucial for improving its robustness. In this paper, combining fixed-time theory criteria, the control strategy of TRICS is extended to fixed-time stability, and the convergence time of the system is not affected by the initial state values.

3) The control schemes proposed in [5–7], [17], and [22] only focus on discussing the steady-state performance of the system, while ignoring its transient performance. This paper combines the key techniques of prescribed performance and command filtering in a backstepping framework to address the issues of differential complexity and singularity, ensuring both steady-state and transient performance of TRICS. This approach optimizes the control performance and system robustness of TRICS, and has significant practical implications.

The rest of this article is organized as follows: Section 2 provides some initial problem descriptions and main theorems. Section 3 presents a design proposal for the NNs observer. Section 4 introduces an adaptive fixed-time control scheme and provides the corresponding stability analysis. Simulation results and the conclusion can be found in Sections 5 and 6, respectively.

## 2. System model descriptions and preliminaries

### 2.1. Twin-roll inclined casting model description

In this subsection, a diagram is presented depicting the twin-roll inclined casting process, as illustrated in Figure 1. Subsequently, a mathematical model of the level of molten steel in the process of twin-roll inclined continuous casting and rolling can be proposed based on [5], as follows:

$$\frac{dy}{dt} = \frac{Q_{in} - Q_{out} - L\Phi(y, x_g, \beta)}{LF(y, x_g, \beta)} \quad (2.1)$$

where  $y$  is the height of molten metal,  $L$  is the surface width of the casting mill roll,  $x_g$  is the roll gap, and  $\beta$  is the inclination angle. The metal inflow quantity  $Q_{in}$  is a nonlinear function of the ladle stopper rod height  $h_s$ , that is,  $Q_{in} = ah_s(b - ch_s)$ , where  $a = 0.2466\pi$ ,  $b = 0.01585$ , and  $c = 0.2165$ . The metal outflow quantity  $Q_{out} = Lx_g\omega R$ , where  $\omega$  represents the angular velocity of the roll's rotation and  $R$  is the radius of roll.

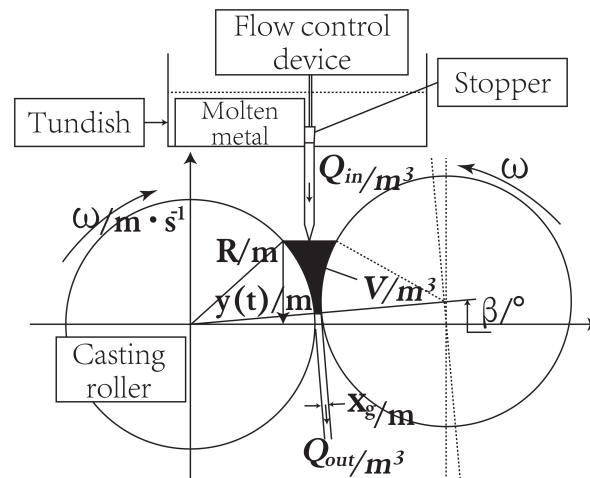


**Figure 1.** Schematic view of the twin-roll inclined casting.

Meanwhile,  $F(y, x_g, \beta)$  and  $\Phi(y, x_g, \beta)$  are defined as the following two nonlinear functions:

$$F(y, x_g, \beta) = (2R + x_g) \cos \beta - \sqrt{R^2 - y^2} - \sqrt{R^2 - (y - (2R + x_g) \sin \beta)^2} \quad (2.2)$$

$$\Phi(y, x_g, \beta) = \left( y \cos \beta + \sin \beta \sqrt{R^2 - (R + \frac{x_g}{2})^2 \sin^2 \beta} - (2R + x_g) \cos \beta \sin \beta \right) \frac{dx_g}{dt} \quad (2.3)$$

Overall, Equation (2.1) can be rewritten as

$$\frac{dy}{dt} = \frac{ah_s(b - ch_s) - Lx_g\omega R - L\Phi(y, x_g, \beta)}{LF(y, x_g, \beta)} \quad (2.4)$$

To develop the control scheme for the subsequent phase, we need to incorporate the coordinate transformations  $x_1 = y$ ,  $x_2 = \frac{dy}{dt}$ , and  $u = h_s$ , which allow us to convert the dynamic equation (2.4) of the molten steel level into a nonaffine nonlinear system in the following format:

$$\begin{cases} \dot{x}_1 = x_2 \\ \dot{x}_2 = f(x, u) + d(t) \\ y = x_1 \end{cases} \quad (2.5)$$

where  $x = [x_1, x_2]^T$  is the state vector of the system, symbols  $u$  and  $y$  represent the control input and output of the system, respectively.  $f(x, u)$  is an unknown nonaffine nonlinear function, and  $d(t)$  represents external disturbance.

**Remark 1:** By taking the derivative of Eq (2.4) of the molten pool level with respect to time  $t$ , we can obtain a strongly coupled unknown smooth nonaffine nonlinear function  $f(x, u)$  and an external

disturbance  $d(t)$ . The function  $f(x, u)$  includes several important time-varying parameters, such as the height of the molten pool level  $y$  and the roll gap opening  $x_g$ , as well as several adjustable parameters, such as the rod height  $h_s$ , roll angular velocity  $\omega$ , and inclination angle  $\beta$ . Meanwhile, the external disturbance  $d(t)$  represents the interference of parameters, such as the angular velocity  $\omega$  and inclination angle  $\beta$  of the casting and rolling rolls, on the casting and rolling effect during the casting and rolling process. This interference is objectively present in practical operations.

Inspired by the decoupling method proposed by Wu in [27] for a class of nonaffine nonlinear system, in order to simplify the difficulty of designing subsequent controllers, the decoupling of the nonaffine nonlinear function  $f(x, u)$  in (2.5) can be obtained using the mean value theorem for derivatives.

$$\begin{aligned} f(x, u) &= f(x, 0) + \frac{\partial f(X, u)}{\partial u} \Big|_{u=u_\varrho} \cdot u \\ &= \tau u + H(x, u) \end{aligned} \quad (2.6)$$

where  $0 < \varrho < 1$ , and  $H(x, u) = (\frac{\partial f(X, u)}{\partial u} \Big|_{u=u_\varrho} \cdot u - \tau)u + f(x, 0)$  where  $\tau > 0$  represents a design parameter. By using (2.6), (2.5) can be rewritten in the following form:

$$\begin{cases} \dot{x}_1 = x_2 \\ \dot{x}_2 = \tau u + H(x, u) + d(t) \\ y = x_1 \end{cases} \quad (2.7)$$

**Control Objective:** The main work of this paper is to design an adaptive NN observer for TRICS with disturbance. By combining prescribed performance and command filtering theory, an adaptive fixed-time controller is developed, such that:

- 1) The constructed observer and controller not only ensure the boundedness of all signals, but also guarantee the fixed-time stability of the CLS.
- 2) The tracking error can be constrained within a predetermined range, thereby ensuring the transient and steady-state performance of the control system.

In order to achieve the desired tracking control objectives, we adopt the following assumptions

**Assumption 1:** The reference signal  $y_r$  and its first-order derivative  $\dot{y}_r$  satisfy  $|y_r| \leq \bar{r}$  and  $|\dot{y}_r| \leq \bar{\dot{r}}$  where  $\bar{r}$  and  $\bar{\dot{r}}$  are unknown positive constants.

**Assumption 2:** For the nonaffine nonlinear term in (2.6), there exist unknown positive constants  $\underline{f}$  and  $\bar{f}$  such that

$$0 < \underline{f} \leq \frac{\partial f(x, u)}{\partial u} \leq \bar{f} \quad (2.8)$$

**Assumption 3:** There exists a positive constant  $\bar{d}$  such that the external disturbance  $|d(t)| < \bar{d}$ .

**Remark 2:** Assumption 1 indicates that the reference signal  $y_r$  and its first-order derivative  $\dot{y}_r$  are bounded, which is essential to demonstrate the boundedness of the virtual control signal and command filter for subsequent designs. Assumption 2 can be used to decouple the nonlinear term in system (2.7), which means that the rate of change of the controlled input gain is bounded. Assumption 3 means that the external disturbance  $d(t)$  is bounded.

## 2.2. Necessary Lemmas preparation

**Definition 1** [28]: Consider a nonlinear system as follows:

$$\dot{x}(t) = g(x, t), x(0) = x_0 \quad (2.9)$$

where  $x$  represents the state variable of the system, and  $g(\cdot)$  is a continuous function with  $g(0, 0) = 0$ . The system (2.9) is practically finite-time stable if there exists a constant  $\gamma > 0$  and a settling time  $T(\gamma, x_0)$  such that  $\|x(t)\| < \gamma$  for all  $t \geq T(\gamma, x_0)$ .

Based on the theory of finite-time stability, if there exists an upper bound  $T_{max} > 0$  in the convergence time such that  $T \leq T_{max}$  and it is not related to the state variables, then the system (2.9) is said to be fixed-time stable.

**Lemma 1** [29]: For the system (2.9), if there exists a positive definite and radial unbounded function  $V(x(t))$  satisfying  $\delta_1\|x(t)\| \leq V(x(t)) \leq \delta_2\|x(t)\|$ , such that

$$\dot{V}(x(t)) \leq -\beta_1 V^p(x(t)) - \beta_2 V^q(x(t)) + \Delta, t \geq 0 \quad (2.10)$$

where  $\delta_1$  and  $\delta_2$  are  $k_\infty$  functions,  $\beta_1 > 0$ ,  $\beta_2 > 0$ ,  $0 < p < 1$ ,  $q > 1$ , and  $\Delta > 0$  are parameters and satisfy  $\Delta < \min\{(1 - \varsigma)\beta_1, (1 - \varsigma)\beta_2\}$  ( $0 < \varsigma < 1$ ), then the non-linear system (2.9) is actually fixed-time stable, and the boundary of its convergence time  $T$  can be expressed as

$$T \leq T_{max} = \frac{1}{\beta_1(1-p)\varsigma} + \frac{1}{\beta_2(q-1)\varsigma} \quad (2.11)$$

**Lemma 2** [30]: For any given positive constants  $m, n$  and  $k$ , and real variables  $x$  and  $y$ , it holds that

$$|x|^m|y|^n \leq \frac{m}{m+n}k|x|^{m+n} + \frac{n}{m+n}k^{-\frac{m}{n}}|y|^{m+n} \quad (2.12)$$

**Lemma 3** [31]: For  $\forall \varpi \geq \nu \geq 0$ , and  $q > 1$ , the following inequality is satisfied:

$$\nu(\varpi - \nu) \leq \frac{q}{q+1}(\varpi^{q+1} - \nu^{q+1}) \quad (2.13)$$

**Lemma 4** [32]: Consider the differential equation in the following form:

$$\dot{\vartheta}(t) = -c_1\vartheta(t) - c_2\vartheta^s(t) + c_3\phi(t) \quad (2.14)$$

where  $c_1 > 0$ ,  $c_2 > 0$ ,  $c_3 > 0$  and  $s = \frac{2m+n}{2m+1} > 1$  ( $m \in N$  and  $n \in N^*$ ) are design constants, and  $\phi(t)$  is a positive function. If the initial condition  $\vartheta(t_0) \geq 0$  holds, then  $\vartheta(t) \geq 0$  for all  $\forall t \geq t_0$ .

## 3. Neural network observer design

In consideration of the limitations in using system state variables for controller design, this section establishes an NN state observer. Subsequently, theory with an adaptive mechanism is designed utilizing the Lyapunov stability analysis method.

Rewrite (2.7) in the form shown below:

$$\begin{cases} \dot{x} = Ax + Ky + B[\tau u + H(x, u) + d(t)] \\ y = Cx \end{cases} \quad (3.1)$$

Selecting an appropriate  $K$  ensures that the matrix  $A$  is a strictly Hurwitz matrix.

Where  $A = \begin{bmatrix} -k_1 & 1 \\ -k_2 & 0 \end{bmatrix}$ ,  $K = \begin{bmatrix} k_1 \\ k_2 \end{bmatrix}$ ,  $B = \begin{bmatrix} 0 \\ 1 \end{bmatrix}$ ,  $C = [1, 0]$ .

The nonlinear function in the expression above can be approximated using radial basis function NNs (RBFNNs), as follows:

$$\begin{aligned} H(x, u|\hat{W}) &= \hat{W}^T \varphi(x, u) \\ H(x, u|W) &= W^T \varphi(x, u) \end{aligned} \quad (3.2)$$

Define  $\hat{W} = [\hat{W}_1, \hat{W}_2, \dots, \hat{W}_l]^T$  and  $(x, u)$  as the weight vector and input vector, respectively.  $\varphi(\cdot) = [\varphi_1, \varphi_2, \dots, \varphi_l]^T$  is the Gaussian function, with  $l$  ( $l > 1$ ) representing the number of nodes in the NNs.

Define the optimal vector  $W$  as

$$W = \arg \min_{\hat{W} \in \Omega_w} [ \sup_{(x, u) \in \Omega_x} |H(x, u) - H(x, u|\hat{W})| ] \quad (3.3)$$

where  $\Omega_w$  and  $\Omega_x$  are the compact sets for  $\hat{W}$  and  $(x, u)$ , respectively. Define  $\epsilon = H(x, u) - H(x, u|W)$ , satisfying  $|\epsilon| \leq \bar{\epsilon}$ , with  $\bar{\epsilon}$  being an unknown positive constant. Then, design the NN state observer as follows:

$$\begin{cases} \dot{\hat{x}} = A\hat{x} + Ky + B[\tau u + H(\hat{x}, u|\hat{W}) + d(t)] \\ y = C\hat{x} \end{cases} \quad (3.4)$$

where  $\hat{x}$  is the estimate of state vector  $x$ , and the observer error is defined as  $e = x - \hat{x} = [e_1, e_2]^T$ .

Therefore, there exist positive definite matrices  $P$  and  $Q$ , such that  $A^T P + P^T A = -2Q$ .

From (3.1) and (3.4), we can obtain

$$\dot{e} = Ae + B[\tilde{W}^T \varphi(\hat{x}, u) + \epsilon] \quad (3.5)$$

where  $\tilde{W} = W - \hat{W}$ . To ensure the boundedness of the state observer (3.4), we choose the Lyapunov function as follow:

$$V_0 = e^T P e \quad (3.6)$$

Then, from (3.6), we have

$$\dot{V}_0 = e^T (A^T P + P A^T) e + 2e^T P B [\tilde{W}^T \varphi(\hat{x}, u) + \epsilon] \quad (3.7)$$

By using Young's inequality, we can calculate

$$2e^T P B \tilde{W}^T \varphi(\hat{x}, u) \leq \|P\|^2 \|e\|^2 + l \tilde{W}^T \tilde{W} \quad (3.8)$$

$$2e^T P B \epsilon \leq \|P\|^2 \|e\|^2 + \bar{\epsilon}^2 \quad (3.9)$$

where  $\varphi(\cdot)$  satisfies  $\varphi^T(\cdot)\varphi(\cdot) \leq l$ . Substituting (3.8) and (3.9) into (3.7) yields:

$$\dot{V}_0 \leq -a\|e\|^2 + l \tilde{W}^T \tilde{W} + \bar{\epsilon}^2 \quad (3.10)$$

where  $a = \lambda_{\min}(Q) - 2\|P\|^2$ .

**Remark 3:** Based on (3.10), we can easily conclude that if the variable  $\tilde{W}$  is bounded, the corresponding observation error  $e$  is also bounded. Thus, we can solve the observer boundedness problem through subsequent stability analysis.

#### 4. Fixed-time controller design and stability analysis

Building upon the previously mentioned NN state observer, we propose a high-performance control scheme that guarantees stability within a fixed time frame. In order to achieve this goal, we have introduced two key technologies: prescribed performance and command filter. The introduction of these technologies is beneficial to the development of our research results.

##### 4.1. Prescribed performance and command filterd method

Prescribed performance control refers to a system in which the system's tracking error converges to a specified small residual set while ensuring good performance in both transient and steady-state. Specifically, the system's convergence rate should be at least a preset value, and its maximum overshoot should be no greater than another preset value. By defining a region enclosed by a performance function, the system achieves prescribed performance control if its tracking error remains within this region.

First, choose a performance function  $\mu(t)$  that is smooth, bounded, and strictly positive.

$$\mu(t) = (\mu_0 - \mu_\infty)e^{-mt} + \mu_\infty \quad (4.1)$$

where  $m > 0$  and  $\mu_0 > \mu_\infty > 0$  are design parameters with  $\mu_0 = \mu(0)$ . Then, introduce a function  $\Psi(\cdot)$  that is smooth, strictly monotonically increasing and ensure  $-\underline{\kappa} < \Psi^{-1} < \bar{\kappa}$ , defined as follows:

$$\Psi(\chi) = \frac{\bar{\kappa}e^\chi - \underline{\kappa}e^{-\chi}}{e^\chi + e^{-\chi}} \quad (4.2)$$

$$\eta = \mu\Psi(\chi)$$

where  $\bar{\kappa} > 0$ ,  $\underline{\kappa} > 0$ , and tracking error  $\eta = x_1 - y_r$ , according to the strictly monotonic increasing property of the function  $\Psi(\chi)$ , the error transformation function  $\chi$  can be expressed as

$$\chi = \Psi^{-1}\left(\frac{\eta}{\mu}\right) = \frac{1}{2} \ln \frac{\Psi + \underline{\kappa}}{\bar{\kappa} - \Psi} \quad (4.3)$$

$$\dot{\chi} = \Pi\left(\dot{\eta} - \frac{\dot{\mu}}{\mu}\eta\right) \quad (4.4)$$

where  $\Pi = \frac{1}{2\mu}\left(\frac{1}{\Psi + \underline{\kappa}} - \frac{1}{\bar{\kappa} - \Psi}\right)$ . Choose appropriate values to satisfy  $-\underline{\kappa}\mu(0) < \eta(0) < \bar{\kappa}\mu(0)$ , which means that the maximum overshoot of the specified  $\eta$  is less than  $\max\{-\underline{\kappa}\mu(0), \bar{\kappa}\mu(0)\}$ .

Combine (4.1) and (4.2) with the selection of appropriate parameters so that the tracking error satisfies the following conditions:

$$-\underline{\kappa}\mu < \eta < \bar{\kappa}\mu \quad (4.5)$$

**Lemma 5:** Consider the tracking error  $\eta$  and the error transformation function  $\chi$  defined in (4.2) and (4.3), respectively. If  $\chi$  is bounded, then it can be guaranteed that the desired performance of  $\eta$ , as stated in (4.5), is satisfied for all  $t > 0$ .

The proof of Lemma 5 will be provided during the stability analysis, which follows.



We combine command filtering and prescribed performance control methods with backstepping design, and introduce the following error coordinate transformation:

$$\begin{aligned} z_1 &= \chi - \frac{1}{2} \ln \frac{\kappa}{\bar{\kappa}} \\ z_2 &= x_2 - \bar{\alpha}_1 \end{aligned} \quad (4.6)$$

where  $\bar{\alpha}_1$  is the output of the first-order command filter for the virtual controller  $\alpha_1$  as

$$\dot{\bar{\alpha}}_1 = \frac{\alpha_1 - \bar{\alpha}_1}{\Sigma}, \bar{\alpha}_1(0) = 0 \quad (4.7)$$

where  $\Sigma$  is a positive design parameter. Similar to [15] and [33], in order to eliminate the error  $\bar{\alpha}_1 - \alpha_1$  caused by filtering, compensation mechanism can be introduced for offsetting.

$$\begin{aligned} \dot{\zeta}_1 &= \Pi(\zeta_2 + \bar{\alpha}_1 - \alpha_1) \\ \dot{\zeta}_2 &= -\Pi\zeta_1 \end{aligned} \quad (4.8)$$

where  $\zeta_i (i = 1, 2)$  is the compensation signal, and  $\zeta_i(0) = 0$ .

#### 4.2. Controller design and stability analysis

In this subsection, we will develop an adaptive fixed-time control scheme for system (2.7) with external disturbance. An adaptive fixed-time controller was designed, which combines backstepping techniques with predetermined performance and command filtering. The controller design process involves two recursive design steps and stability analysis is conducted on it using Lyapunov stability theory.

Define the compensating filtering error as

$$v_i = z_i - \zeta_i \quad (i = 1, 2) \quad (4.9)$$

**Step 1:** Constructing the Lyapunov function as  $V_1 = V_0 + \frac{1}{2}v_1^2$ . From (4.6) and (4.9), the time derivative of  $V_1$  yields

$$\begin{aligned} \dot{V}_1 &= \dot{V}_0 + v_1\dot{v}_1 \\ &= \dot{V}_0 + v_1(\dot{z}_1 - \dot{\zeta}_1) \\ &\leq \dot{V}_0 + \Pi v_1(x_2 - \dot{y}_r - \frac{\dot{\mu}}{\mu}\eta - \xi_2 - \bar{\alpha}_1 + \alpha_1) \\ &\leq \dot{V}_0 + \Pi(v_2 + \alpha_1 - \dot{y}_r - \frac{\dot{\mu}}{\mu}\eta) \end{aligned} \quad (4.10)$$

Choose the following virtual control function  $\alpha_1$ :

$$\alpha_1 = -\frac{\lambda_1}{\Pi}v_1^{2p-1} - \frac{\iota_1}{\Pi}v_1^{2q-1} + \dot{y}_r + \frac{\dot{\mu}}{\mu}\eta \quad (4.11)$$

where  $0 < p < 1$ ,  $q = \frac{2m+n}{2m+1} > 1$  ( $m \in N$  and  $n \in N^*$ ),  $\lambda_1 > 0$  and  $\iota_1 > 0$  are design parameters.

By using (4.10) and (4.11), the following can be obtained:

$$\begin{aligned} \dot{V}_1 &\leq -a\|e\|^2 + l\tilde{W}^T\tilde{W} - \lambda_1v_1^{2p} - \iota_1v_1^{2q} \\ &\quad + \Pi v_1 v_2 + \bar{\epsilon}^2 \end{aligned} \quad (4.12)$$

**Step 2:** Taking the derivative of  $v_2$  with respect to time yields

$$\begin{aligned}
 \dot{v}_2 &= \dot{z}_2 - \dot{\zeta}_2 \\
 &= \dot{x}_2 - \dot{\bar{\alpha}}_1 + \Pi\zeta_1 \\
 &= \tau u + H(\hat{x}, u) + d(t) - \frac{\alpha_1 - \bar{\alpha}_1}{\Sigma} + \Pi\zeta_1 \\
 &= \tau u + \hat{W}^T \varphi(\hat{x}, u) + \epsilon + \tilde{W}^T \varphi(\hat{x}, u) \\
 &\quad + d(t) - \frac{\alpha_1 - \bar{\alpha}_1}{\Sigma} + \Pi\zeta_1
 \end{aligned} \tag{4.13}$$

Choose the following Lyapunov function  $V_2$ :

$$V_2 = V_1 + \frac{1}{2}v_2^2 + \frac{l}{2\Gamma} \tilde{W}^T \tilde{W} \tag{4.14}$$

where  $\Gamma$  is a positive design parameter.

The time differentiation of (4.14) can be represented as

$$\begin{aligned}
 \dot{V}_2 &= \dot{V}_1 + v_2 \dot{v}_2 - \frac{l}{\Gamma} \tilde{W} \dot{\tilde{W}} \\
 &\leq \dot{V}_1 + v_2(\tau u + \hat{W}^T \varphi(\hat{x}, u) + \tilde{W}^T \varphi(\hat{x}, u) \\
 &\quad + \epsilon + d(t) - \frac{\alpha_1 - \bar{\alpha}_1}{\Sigma} + \Pi\zeta_1) - \frac{l}{\Gamma} \tilde{W} \dot{\tilde{W}}
 \end{aligned} \tag{4.15}$$

By utilizing the Young's inequality, we obtain

$$v_2(\epsilon + d(t)) \leq v_2^2 + \frac{1}{2}\bar{\epsilon}^2 + \frac{1}{2}\bar{d}^2 \tag{4.16}$$

Design the following fixed-time controller  $u$  and adaptive law  $W$ :

$$u = \frac{1}{\tau} \left( -v_2 - \hat{W}^T \varphi(\hat{x}, u) - \lambda_2 v_2^{2p-1} - \iota_2 v_2^{2q-1} + \frac{\alpha_1 - \bar{\alpha}_1}{\Sigma} - \Pi\zeta_1 \right) \tag{4.17}$$

$$\dot{\hat{W}} = \Gamma v_2 \varphi(\hat{x}, u) - \sigma \hat{W} - \iota \hat{W}^{2q-1}, \hat{W}(0) \geq 0 \tag{4.18}$$

where  $\lambda_2$ ,  $\iota_2$ ,  $\sigma$ , and  $\iota$  are positive design parameters.

To ensure the stability of the system within a fixed-time, the adaptive law (4.18) needs to be designed in the form of nonlinear differential equations similar to those in Lemma 4. A detailed proof of Lemma 4 is provided in [31]. Adopting this method can assist in proving, in the subsequent stability analysis, that the system described by (2.7) satisfies the criterion for fixed-time stability in Lemma 1.

Thus, this article's primary outcome for the stabilization theorem of closed-loop nonlinear system is summarized as

**Theorem 1:** Consider the nonlinear system (2.7) with disturbance, under Assumptions 1–3, if choosing the adaptive NN state observer (3.4), the adaptive fixed-time controller (4.17), the virtual control function (4.11), and the adaptive law (4.18), the following conclusions can be drawn:

1) The nonlinear system (2.7) is fixed-time stable, and the upper bound on the settling time is

$$T \leq T_{max} = \frac{100}{\beta_1(1-p)} + \frac{100}{\beta_2(q-1)} \tag{4.19}$$

The coefficients  $\beta_1$  and  $\beta_2$  will be calculated in the forthcoming section of the proof.

2) Within a fixed-time period, the tracking error can be limited to a predetermined set. That is, for time  $t \geq 0$ , the condition  $-\underline{\kappa}\mu < \eta < \bar{\kappa}\mu$  is satisfied. Additionally, all signals of the closed loop system (CLS) are still bounded.

**Proof:** Substituting (4.12) and (4.16)–(4.18) into (4.15) and carrying out some computations, one has

$$\begin{aligned} \dot{V}_2 \leq & -a\|e\|^2 + l\tilde{W}^T\tilde{W} - \sum_{i=1}^2 \lambda_i v_i^{2p} - \sum_{i=1}^2 \iota_i v_i^{2q} \\ & + \frac{l\sigma}{\Gamma} \tilde{W}\hat{W} + \frac{h}{\Gamma} \tilde{W}\hat{W}^{2q-1} + \Delta \end{aligned} \quad (4.20)$$

where  $\Delta = \bar{\epsilon}^2 + \frac{1}{2}\bar{d}^2$ .

Utilizing the Young's inequality yields

$$\tilde{W}\hat{W} = \tilde{W}(W - \tilde{W}) \leq -\frac{1}{2}\tilde{W}^T\tilde{W} + \frac{1}{2}W^2 \quad (4.21)$$

Based on Lemma 4 and (4.18), it can be inferred that  $\hat{W} \geq 0$  is satisfied for all  $\forall t \geq t_0$ . Furthermore, by Lemma 3, we have

$$\begin{aligned} \tilde{W}\hat{W}^{2q-1} &= \tilde{W}(W - \tilde{W})^{2q-1} \\ &\leq \frac{2q-1}{2q}(W^{2q} - \tilde{W}^{2q}) \end{aligned} \quad (4.22)$$

For Lemma 2, if we let  $x = \frac{l}{2\Gamma}\tilde{W}^T\tilde{W}$ ,  $y = 1$ ,  $m = p$ ,  $n = 1 - p$ , and  $k = \frac{1}{p}$ , then we can obtain the following inequality:

$$\left(\frac{l}{2\Gamma}\tilde{W}^T\tilde{W}\right)^p \leq \frac{l}{2\Gamma}\tilde{W}^T\tilde{W} + (1-p)p^{\frac{p}{1-p}} \quad (4.23)$$

Likewise, can derive (4.24) and (4.25)

$$\|e\|^{2p} \leq \|e\|^2 + (1-p)p^{\frac{p}{1-p}} \quad (4.24)$$

$$\|e\|^{2q} \leq \|e\|^2 + (1-q)q^{\frac{q}{1-q}} \quad (4.25)$$

In the light of formulas (4.21)–(4.25), we have

$$\begin{aligned}
 \dot{V}_2 &\leq -\frac{a}{2}\|e\|^{2p} - \frac{a}{2}\|e\|^{2q} - \sum_{i=1}^2 \lambda_i v_i^{2p} \\
 &\quad - \sum_{i=1}^2 \iota_i v_i^{2q} - (\sigma - 2\Gamma) \left(\frac{l}{2\Gamma} \tilde{W}^T \tilde{W}\right)^p \\
 &\quad - 2^q l^{1-q} \Gamma^{q-1} \iota \frac{2q-1}{2q} \left(\frac{l}{2\Gamma} \tilde{W}^T \tilde{W}\right)^q + \check{\Delta} \\
 &\leq -\frac{a}{2}(\|e\|^2)^p - \frac{a}{2}(\|e\|^2)^q - \sum_{i=1}^2 2^p \lambda_i \left(\frac{v_i^2}{2}\right)^p \\
 &\quad - \sum_{i=1}^2 2^p \iota_i \left(\frac{v_i^2}{2}\right)^q - (\sigma - 2\Gamma) \left(\frac{l}{2\Gamma} \tilde{W}^T \tilde{W}\right)^p \\
 &\quad - \frac{2\Gamma \iota}{l} \left(\frac{l}{2\Gamma} \tilde{W}^T \tilde{W}\right)^q + \check{\Delta} \\
 &\leq -\beta_1 V_2^p - \beta_2 V_2^q + \check{\Delta}
 \end{aligned} \tag{4.26}$$

where  $\beta_1 = \min\{\frac{a}{2}, 2^p \lambda_i, \sigma - 2\Gamma, i = 1, 2\}$ ,  $\beta_2 = \min\{\frac{a}{2}, 2^p \iota_i, \frac{2\Gamma \iota}{l}, i = 1, 2\}$ ,  $\check{\Delta} = \Delta + (\sigma - 2\Gamma + \frac{a}{2})(1 - p)p^{\frac{p}{1-p}} + \frac{a}{2}(1 - q)q^{\frac{q}{1-q}} + \frac{l}{\Gamma} \frac{2q-1}{2q} W^{2q} + \frac{l\sigma}{\Gamma} W^2$ .

From (4.26), we can see that we only need to let  $\sigma - 2\Gamma > 0$  to conclude that both  $v_i$  and  $\tilde{W}$  are bounded, and the proof of the boundedness of  $\zeta_i$  has been given in [15] and [33]. Thus, the boundedness of  $z_i$  can be inferred by means of (4.9). Furthermore, using the error transformation (4.3), we can demonstrate that  $\chi$  remains bounded.

In summary, the proof of Lemma 5 is presented as follows.

Since  $\chi$  is bounded, there exist constants  $\underline{\chi}$  and  $\bar{\chi}$  such that  $\underline{\chi} < \chi < \bar{\chi}$  holds for  $t \geq 0$ . By using  $\eta = \mu\Psi(\chi)$ , one has

$$\Psi(\underline{\chi})\mu < \eta < \Psi(\bar{\chi})\mu, t \geq 0 \tag{4.27}$$

Then, from the fact that  $-\underline{\kappa} < \Psi^{-1} < -\bar{\kappa}$ , we obtain

$$-\underline{\kappa}\mu < \eta < \bar{\kappa}\mu, \forall t \geq 0 \tag{4.28}$$

The performance of  $\eta$  as prescribed in (4.5) is achieved for  $\forall t \geq 0$ .

The proofs of Theorem 1 and Lemma 5 are complete.

**Remark 4:** From Lemma 1 and (4.26), the nonlinear system (2.7) is proven to be fixed-time stable and the settling time  $T$  is restricted by (4.19). The boundary of the set time  $T$ , independent of initial conditions, is evident from (4.19). Furthermore, the tracking error can converge within a predetermined range that is within  $T_{max}$ . Different time boundaries can be set by adjusting the parameters according to performance requirements in advance, without imposing any conditions on the initial state. Therefore, in comparison to the existing adaptive control methods for TRICS discussed in the current literature, the proposed control scheme in this paper can ensure both the steady-state and transient performance of the TRICS, which holds great significance in practical engineering applications.

**Remark 5:** It is noteworthy that the design process of the latter step in the traditional backstepping process necessitates utilizing the derivative of the virtual control function constructed in the previous

step. When differentiating the virtual control (designed in Eq (4.11)), the  $\frac{\lambda_1}{\Pi} v_1^{2p-2}$  is calculated by the first term (i.e.,  $\frac{\lambda_1}{\Pi} v_1^{2p-1}$ ). If  $2p - 2 < 0$ , a singularity may appear. To address this issue, we have introduced the command filter control method in the backstepping step, which obviates the necessity of calculating the first-order derivative of the virtual control law  $\alpha_1$  and avoids the singularity problem.

Given the results presented in this article, in order to facilitate understanding, the control flow diagram of TRICS is provided as shown in Figure 2.

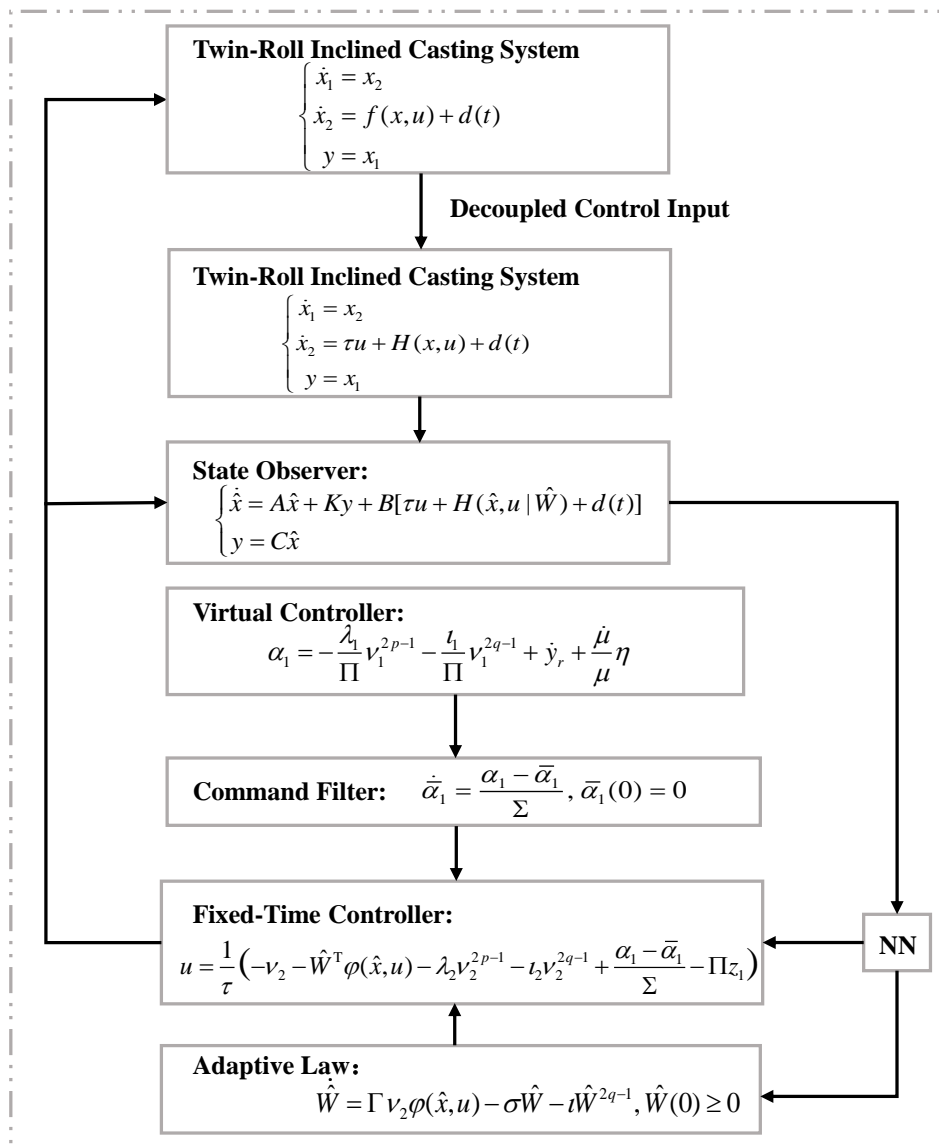


Figure 2. Block diagram of TRICS.

## 5. Simulation results

In this section, the effectiveness of the developed controller for TRICS with disturbance was verified through a simulation example.

To facilitate the simulation, the design parameters utilized in the control scheme are presented in Table 1. The corresponding system parameters are selected as  $R = 150 \text{ mm}$ ,  $L = 200 \text{ mm}$ ,  $\omega = 170 \text{ mm/s}$  and  $\beta = 5^\circ$ . The chosen reference signal for tracking is  $y_r = \sin(t)$ , and the external disturbance is  $d(t) = 0.1\cos(t)$ . For the performance function in (4.1), select  $\mu_0 = 2.8$ ,  $\mu_\infty = 0.1$ , and  $m = \underline{\kappa} = \bar{\kappa} = 1$ , yielding  $\mu(t) = 2.7e^{-t} + 0.1$ .

In Table 2, two groups of initial values for different systems are provided. Among them,  $x_i$  ( $i = 1, 2$ ) represents the state variables ( $x_2$  represents the unmeasurable state). Meanwhile, state variables  $x_1$  and  $x_2$  respectively correspond to the level of molten steel and the rate of change of the level of molten steel in TRICS.

**Table 1.** Design parameters.

Parameters	Values	Parameters	Values
$\lambda_1, \lambda_2$	12, 30	$\Gamma, \sigma$	2, 10
$\iota_1, \iota_2, \iota$	15, 25, 20	$p, q$	$\frac{99}{101}, \frac{102}{99}$
$k_1, k_2$	25, 300	$\Sigma$	0.2

**Table 2.** Initial values.

Initial states of system	Initial values in case 1	Initial values in case 2
$x_1(0), x_2(0)$	0.2, 0.2	-0.5, 0.2
$\hat{x}_1(0), \hat{x}_2(0)$	-0.2, -0.2	-0.3, 0.5
$\hat{W}(0), \bar{\alpha}_1(0)$	0.15, 0	0.4, 0
$\zeta_1(0), \zeta_2(0)$	0, 0	0, 0

In addition, all basis functions are selected as Gaussian functions, which include 11 nodes. These nodes are evenly spaced between  $-5$  and  $5$ , with a width of  $0.5$  for each node.

Based on the definition of parameters  $\beta_1$  and  $\beta_2$  in the above design parameters and inequality (4.19), we can obtain  $T \leq T_{max} \leq 1295 \text{ s}$  and can set the upper limit of the settling time by adjusting the control parameters.

The simulation results are shown in Figures 3–8. Figure 3 shows the trajectories of the system states  $x_i$  ( $i = 1, 2$ ) and observer states  $\hat{x}_i$  ( $i = 1, 2$ ) in case 1. Figure 4 plots the trajectories of  $\eta$  and  $\hat{W}$  in case 1. Figure 5 displays the curves of control input  $u$  in case 1. Figure 6 plots the trajectories of  $x_i$  ( $i = 1, 2$ ) and  $\hat{x}_i$  ( $i = 1, 2$ ) in case 2. Figure 7 plots the trajectories of  $\eta$  and  $\hat{W}$  in case 2. Figure 8 plots the trajectory of  $u$  in case 2.

From Figures 3 and 6, it can be seen that the designed NN observer is capable of effectively estimating unmeasurable states. Figures 3–8 validate that both sets of different initial values can ensure excellent system performance, with the upper limit of the convergence time unaffected by the initial system state, while also able to quickly limit the tracking error within the predetermined boundaries. This further demonstrates the effectiveness of the proposed control scheme in this paper. The simulation results indicate that the control strategy designed for TRICS in this paper is feasible.

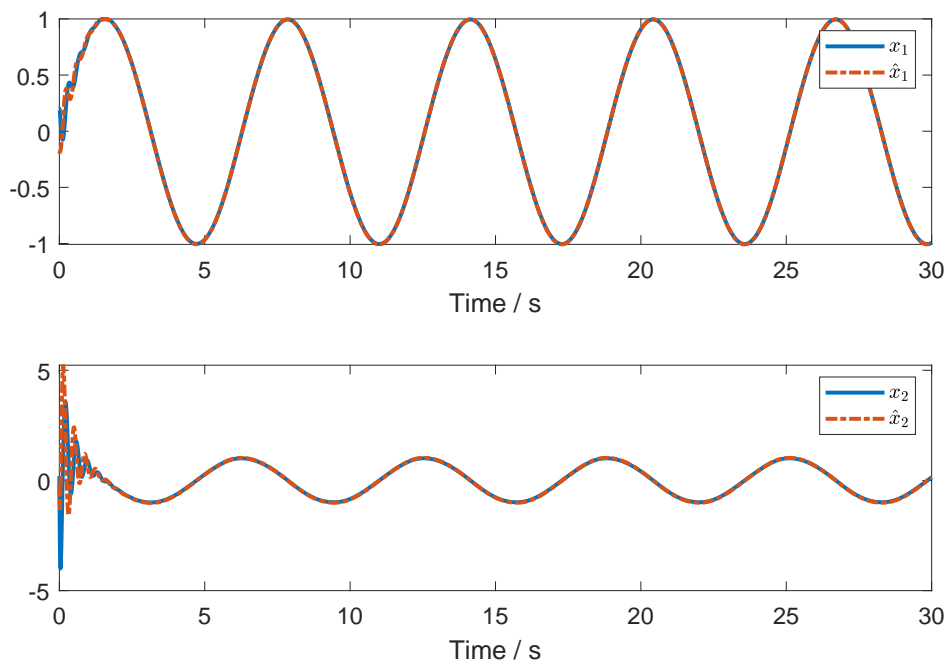


**Figure 3.** System states  $x_i$  ( $i = 1, 2$ ) and observer states  $\hat{x}_i$  ( $i = 1, 2$ ) in case 1.

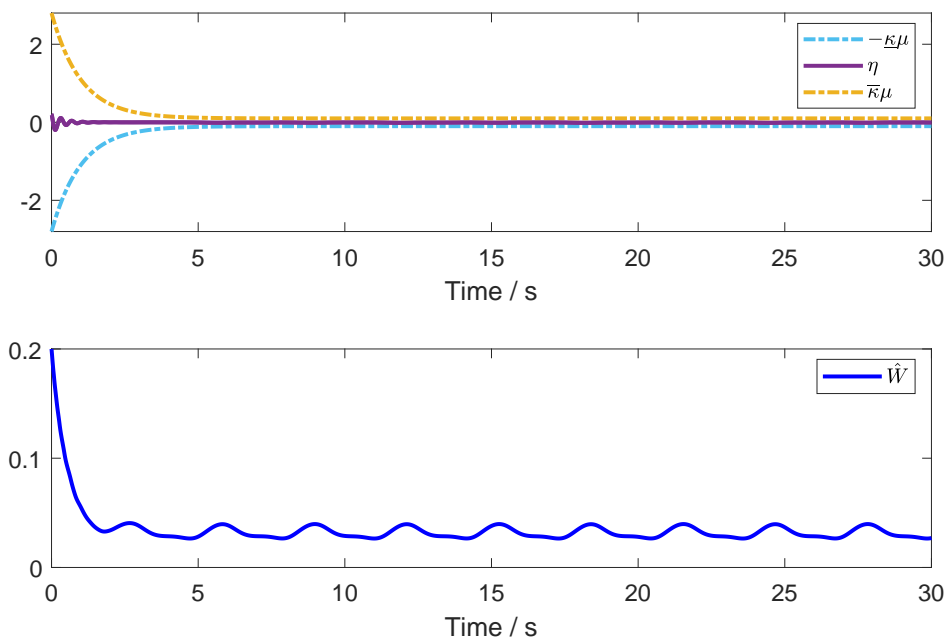


**Figure 4.** Trajectories of  $\eta$  and  $\hat{W}$  in case 1.

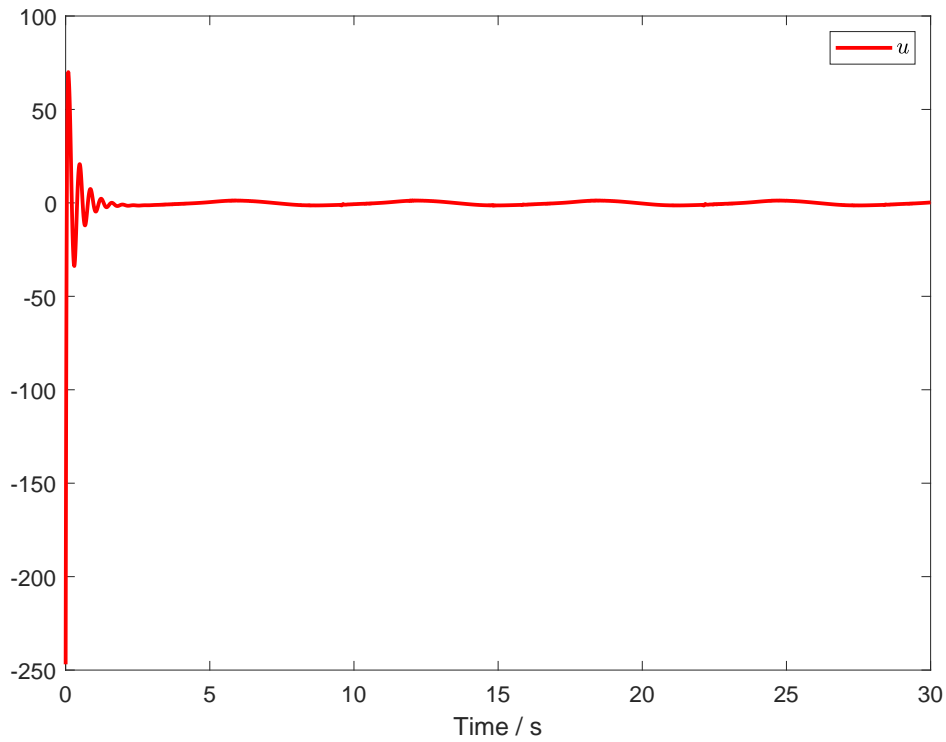


**Figure 5.** System control input  $u$  in case 1.

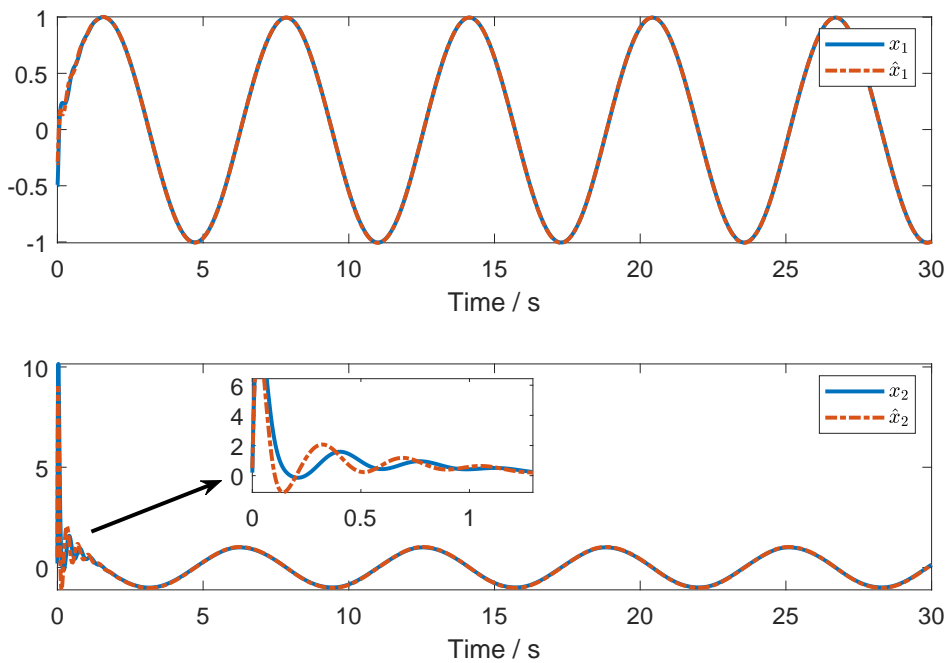


**Figure 6.** System states  $x_i$  ( $i = 1, 2$ ) and observer states  $\hat{x}_i$  ( $i = 1, 2$ ) in case 2.



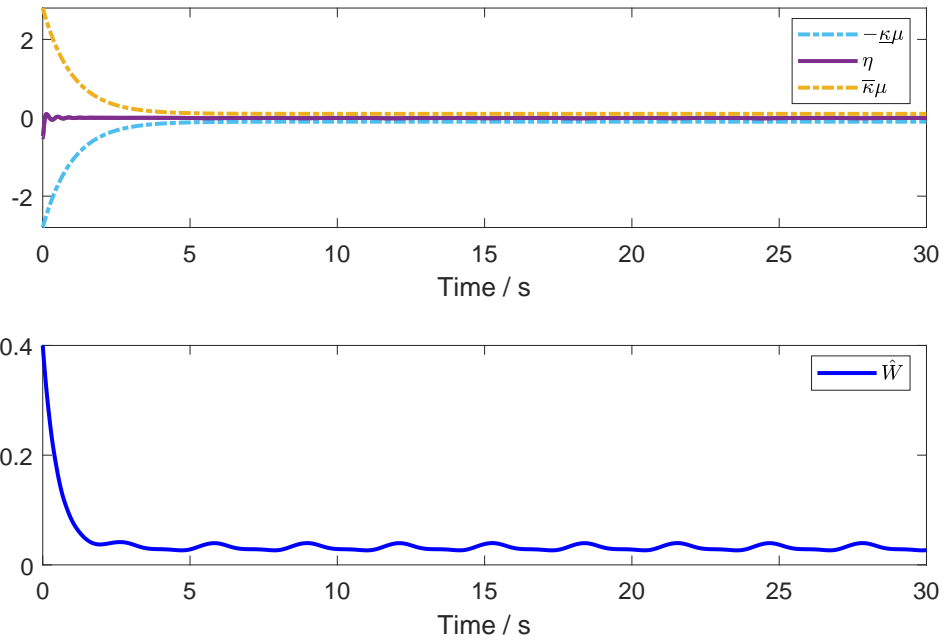


**Figure 7.** Trajectories of  $\eta$  and  $\hat{W}$  in case 2.

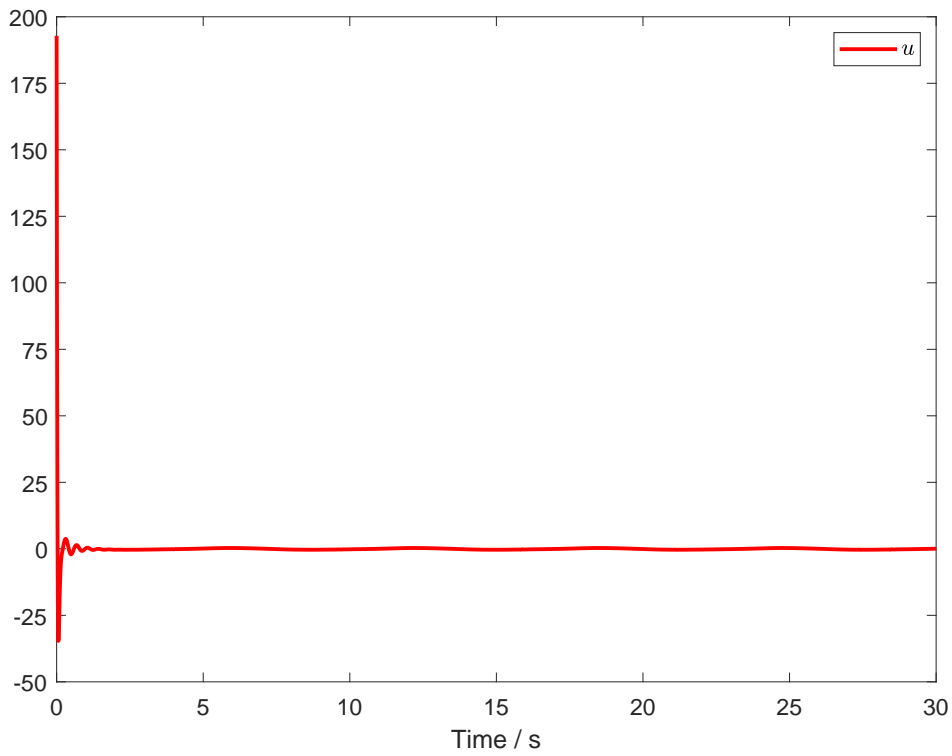


**Figure 8.** System control input  $u$  in case 2.

## 6. Conclusions

The proposed adaptive output feedback fixed-time control strategy in this paper provides an effective solution for optimizing the performance of TRICS with external disturbance. This method can effectively estimate the observed state while avoiding the complexity and singularity issues in traditional backstepping methods. Simulation results show that this strategy not only guarantees that the signals in the closed-loop system are fixed-time bounded, but also achieves fast tracking of the molten pool level, with good transient and steady-state performance. Therefore, this method plays an important role in improving the overall performance of the process and has the potential for practical applications. In the future, efforts will be made to extend the control scheme to handle more complex scenarios and explore the application of the proposed approach in other industrial processes with similar control challenges.

### Use of AI tools declaration

The authors declare they have not used Artificial Intelligence (AI) tools in the creation of this article.

### Acknowledgments

This work was supported in part by the Natural Science Foundation of Liaoning Province of China under Grant 2022-MS-356.

### Conflict of interest

The authors declare there is no conflict of interest.

### References

1. Z. Yu, Z. S. Lei, Q. S. Li, K. Deng, Z. M. Ren, Physical simulation of nozzle electromagnetic brake in twin-roll strip casting, *Steel Res. Int.*, **79** (2008), 839–842. <https://doi.org/10.1002/srin.200806208>
2. S. Ge, M. Isac, R. I. L. Guthrie, Progress of strip casting technology for steel; historical developments, *ISIJ Int.*, **52** (2012), 2109–2122. <https://doi.org/10.2355/isijinternational.52.2109>
3. M. Vidoni, M. Daamen, G. Hirt, Advances in the twin-roll strip casting of strip with profiled cross section, *Key Eng. Mater.*, **554** (2013), 562–571. <https://doi.org/10.4028/www.scientific.net/kem.554-557.562>
4. T. Haga, Y. Kurahashi, Casting process at roll bite in strip cast using vertical-type high-speed twin-roll caster, *Metals*, **12** (2022), 1169. <https://doi.org/10.3390/met12071169>
5. Y. J. Zhang, L. B. Wu, H. Y. Zhao, X. D. Hu, W. Y. Zhang, D. Y. Ju, Robust adaptive fuzzy output tracking control for a class of twin-roll strip casting systems, *Math. Probl. Eng.*, **2017** (2017). <https://doi.org/10.1155/2017/6742630>
6. D. X. Gao, Y. J. Zhang, L. B. Wu, S. H. Liu, Adaptive neural command filtered fault-tolerant control for a twin roll inclined casting system, *Metalurgija*, **62** (2023), 355–358.

7. D. X. Gao, Y. J. Zhang, L. B. Wu, S. H. Liu, Mathematical modeling and command filter adaptive fuzzy control based on twin-roll inclined strip casting process, *J. Control Autom. Electr. Syst.*, **34** (2023), 1220–1230. <https://doi.org/10.1007/s40313-023-01029-x>
8. L. Liu, Y. J. Liu, S. C. Tong, Z. W. Gao, Relative threshold-based event-triggered control for nonlinear constrained systems with application to aircraft wing rock motion, *IEEE Trans. Ind. Inf.*, **18** (2021), 911–921. <https://doi.org/10.1109/tii.2021.3080841>
9. Y. J. Liu, M. Z. Gong, S. C. Tong, C. L. P. Chen, D. J. Li, Adaptive fuzzy output feedback control for a class of nonlinear systems with full state constraints, *IEEE Trans. Fuzzy Syst.*, **26** (2018), 2607–2617. <https://doi.org/10.1109/TFUZZ.2018.2798577>
10. Y. X. Li, G. H. Yang, Observer-based fuzzy adaptive event-triggered control codesign for a class of uncertain nonlinear systems, *IEEE Trans. Fuzzy Syst.*, **26** (2017), 1589–1599. <https://doi.org/10.1109/TFUZZ.2017.2735944>
11. Y. X. Li, S. C. Tong, G. H. Yang, Observer-based adaptive fuzzy decentralized event-triggered control of interconnected nonlinear system, *IEEE Trans. Cybern.*, **50** (2019), 3104–3112. <https://doi.org/10.1109/TCYB.2019.2894024>
12. L. Liu, Y. J. Cui, Y. J. Liu, S. C. Tong, Observer-based adaptive neural output feedback constraint controller design for switched systems under average dwell time, *IEEE Trans. Cybern.*, **68** (2021), 3901–3912. <https://doi.org/10.1109/TCSI.2021.3093326>
13. F. Shen, X. J. Wang, X. H. Yin, Adaptive neural output-feedback tracking control for a class of stochastic nonlinear systems with output constraint and unknown control coefficients, *Int. J. Robust Nonlinear Control*, **32** (2022), 1862–1878. <https://doi.org/10.1002/rnc.5918>
14. S. P. Bhat, D. S. Bernstein, Continuous finite-time stabilization of the translational and rotational double integrators, *IEEE Trans. Autom. Control*, **43** (1998), 678–682. <https://doi.org/10.1109/9.668834>
15. Y. X. Li, Finite time command filtered adaptive fault tolerant control for a class of uncertain nonlinear systems, *Automatica*, **106** (2019), 117–123. <https://doi.org/10.1016/j.automatica.2019.04.022>
16. J. L. Sun, H. B. He, J. Q. Yi, Z. Q. Pu, Finite-time command-filtered composite adaptive neural control of uncertain nonlinear systems, *IEEE Trans. Cybern.*, **52** (2020), 6809–6821. <https://doi.org/10.1109/TCYB.2020.3032096>
17. C. Wang, C. Zhang, D. He, J. L. Xiao, L. Y. Liu, Observer-based finite-time adaptive fuzzy backstepping control for mimo coupled nonlinear systems, *Math. Biosci. Eng.*, **19** (2022), 10637–10655. <https://doi.org/10.3934/mbe.2022497>
18. F. Wang, B. Chen, Y. M. Sun, Y. L. Gao, C. Lin, Finite-time fuzzy control of stochastic nonlinear systems, *IEEE Trans. Cybern.*, **50** (2019), 2617–2626. <https://doi.org/10.1109/TCYB.2019.2925573>
19. P. H. Du, H. J. Liang, S. Y. Zhao, C. K. Ahn, Neural-based decentralized adaptive finite-time control for nonlinear large-scale systems with time-varying output constraints, *IEEE Trans. Syst. Man Cybern. Syst.*, **51** (2019), 3136–3147. <https://doi.org/10.1109/TSMC.2019.2918351>
20. A. Polyakov, Nonlinear feedback design for fixed-time stabilization of linear control systems, *IEEE Trans. Autom. Control*, **57** (2011), 2106–2110. <https://doi.org/10.1109/TAC.2011.2179869>

21. M. Chen, H. Q. Wang, X. P. Liu, Adaptive fixed-time stabilization for a class of nonlinear uncertain systems, *IEEE Trans. Fuzzy Syst.*, **29** (2019), 664–673. <https://doi.org/10.1109/TFUZZ.2019.2959972>
22. Y. Zhao, J. L. Yao, J. Tian, J. B. Yu, Adaptive fixed-time stabilization for a class of nonlinear uncertain systems, *Math. Biosci. Eng.*, **20** (2023), 8241–8260. <https://doi.org/10.3934/mbe.2023359>
23. L. L. Zhang, L. C. Zhu, C. C. Hua, C. Qian, Fixed-time observer-based output feedback control for nonlinear systems with full-state constraints, *IEEE Trans. Circuits Syst. II Express Briefs*, **2022** (2022). <https://doi.org/10.1109/TCSII.2022.3224957>
24. Q. Liang, Q. M. Yang, W. C. Meng, Y. P. Li, Adaptive finite-time control for turbo-generator of power systems with prescribed performance, *Asian J. Control*, **24** (2022), 1597–1608. <https://doi.org/10.1002/asjc.2553>
25. H. D. Shan, H. Xue, S. L. Hu, H. J. Liang, Finite-time dynamic surface control for multi-agent systems with prescribed performance and unknown control directions, *Int. J. Syst. Sci.*, **53** (2022), 325–336. <https://doi.org/10.1080/00207721.2021.1954719>
26. Z. G. Zhou, D. Zhou, X. N. Shi, R. F. Li, B. Q. Kan, Prescribed performance fixed-time tracking control for a class of second-order nonlinear systems with disturbances and actuator saturation, *Int. J. Control*, **94** (2021), 223–234. <https://doi.org/10.1080/00207179.2019.1590644>
27. L. B. Wu, G. H. Yang, Adaptive fault-tolerant control of a class of nonaffine nonlinear systems with mismatched parameter uncertainties and disturbances, *Nonlinear Dyn.*, **82** (2015), 1281–1291. <https://doi.org/10.1007/s11071-015-2235-6>
28. H. Y. Li, S. Y. Zhao, W. He, R. Q. Lu, Adaptive finite-time tracking control of full state constrained nonlinear systems with dead-zone, *Automatica*, **100** (2019), 99–107. <https://doi.org/10.1016/j.automatica.2018.10.030>
29. H. Q. Wang, J. W. Ma, X. D. Zhao, B. Niu, M. Chen, W. Wang, Adaptive fuzzy fixed-time control for high-order nonlinear systems with sensor and actuator faults, *IEEE Trans. Fuzzy Syst.*, **31** (2023), 2658–2668. <https://doi.org/10.1109/TFUZZ.2023.3235395>
30. S. Furuichi, N. Minculete, Alternative reverse inequalities for young’s inequality, *J. Math. Inequal.*, **5** (2011), 595–600.
31. F. Wang, G. Y. Lai, Fixed-time control design for nonlinear uncertain systems via adaptive method, *Syst. Control Lett.*, **140** (2020), 104704. <https://doi.org/10.1016/j.sysconle.2020.104704>
32. Y. Zhang, F. Wang, Observer-based fixed-time neural control for a class of nonlinear systems, *IEEE Trans. Neural Netw. Learn. Syst.*, **33** (2021), 2892–2902. <https://doi.org/10.1109/TNNLS.2020.3046865>
33. Y. X. Li, Command filter adaptive asymptotic tracking of uncertain nonlinear systems with time-varying parameters and disturbances, *IEEE Trans. Autom. Control*, **67** (2021), 2973–2980. <https://doi.org/10.1109/TAC.2021.3089626>

